European Spine Journal
https://doi.org/10.1007/s00586-018-5704-z

ORIGINAL ARTICLE

Population-averaged MRI atlases for automated image processing and assessments of lumbar paraspinal muscles

Yiming Xiao[1] · **Maryse Fortin**[2] · **Michele C. Battié**[3,4] · **Hassan Rivaz**[2,5]

Received: 22 March 2018 / Accepted: 16 July 2018

Abstract

Purpose Growing evidence suggests an association between lumbar paraspinal muscle degeneration and low back pain (LBP). Currently, time-consuming and laborious manual segmentations of paraspinal muscles are commonly performed on magnetic resonance imaging (MRI) axial scans. Automated image analysis algorithms can mitigate these drawbacks, but they often require individual MRIs to be aligned to a standard "reference" atlas. Such atlases are well established in automated neuroimaging analysis. Our aim was to create atlases of similar nature for automated paraspinal muscle measurements.

Methods Lumbosacral T2-weighted MRIs were acquired from 117 patients who experienced LBP, stratified by gender and age group (30–39, 40–49, and 50–59 years old). Axial MRI slices of the L4–L5 and L5–S1 levels at mid-disc were obtained and aligned using group-wise linear and nonlinear image registration to produce a set of unbiased population-averaged atlases for lumbar paraspinal muscles.

Results The resulting atlases represent the averaged morphology and MRI intensity features of the corresponding cohorts. Differences in paraspinal muscle shapes and fat infiltration levels with respect to gender and age can be visually identified from the population-averaged data from both linear and nonlinear registrations.

Conclusion We constructed a set of population-averaged atlases for developing automated algorithms to help analyze paraspinal muscle morphometry from axial MRI scans. Such an advancement could greatly benefit the fields of paraspinal muscle and LBP research.

Graphical abstract These slides can be retrieved under Electronic Supplementary Material.

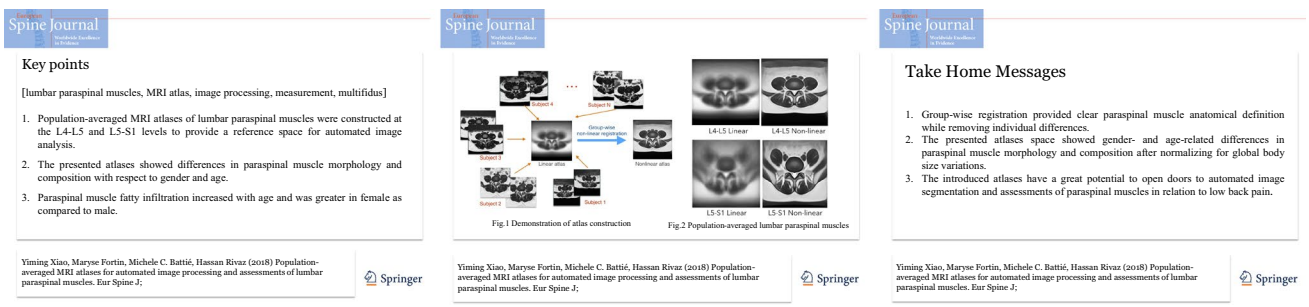

Keywords Lumbar paraspinal muscles · MRI atlas · Image processing · Measurement · Multifidus

Introduction

With a lifetime prevalence of up to 84%, low back pain (LBP) is the most common musculoskeletal disorder in adults [1] and causes enormous economic burden on individuals, family, and governments. While conditions such

Electronic supplementary material The online version of this article (https://doi.org/10.1007/s00586-018-5704-z) contains supplementary material, which is available to authorized users.

✉ Yiming Xiao
yxiao286@uwo.ca

Extended author information available on the last page of the article

Published online: 26 July 2018

as lumbar spinal stenosis and disc herniation can result in LBP, the underlying pathology remains unknown in the vast majority of patients seeking care [2]. Most LBP is considered self-limited, but evidence suggests that a high portion of patients develop recurrent symptoms, resulting in poor functional outcomes and additional medical treatments [3].

To improve the understanding of LBP pathology and prognosis, as well as developing appropriate treatment and rehabilitation strategies, there is a growing interest in investigating the association between LBP and lumbar paraspinal muscle atrophy, fatty infiltration, and abnormal anatomical asymmetries shown on magnetic resonance imaging (MRI) scans [4–6]. Previous case–control studies have suggested that LBP and lumbar pathology are associated with smaller muscle size or more fatty infiltration when contrasting those with symptoms to healthy controls [7, 8], although findings have not been entirely consistent. Such muscle measures are also influenced by other factors, such as physiological changes due to natural aging and sex differences, complicating analyses of associations with pain and pathology [9, 10].

In practice, axial slices obtained from lumbar spinal MRI are often used to perform muscle measurements since muscle cross-sectional area (CSA) is commonly viewed as an indicator for muscle force production capacity, and fatty infiltration and left-and-right asymmetry can also be gauged [8]. To date, almost all related studies [4, 5, 7–9] have used qualitative measurements or manual segmentation to measure variation in muscle morphology and composition. While manual segmentation allows quantitative muscle measures, it is a time-consuming and arduous procedure. In addition, inter- and intra-rater variability can affect the quality of analysis. Fully automated imaging analysis algorithms, including image segmentation, can improve the efficiency and consistency of muscle morphometry and composition measurements, potentially yielding more insightful results. However, so far, very few semi- or fully automated algorithms [11] have been proposed. To take advantage of computer-assisted image analysis, individual MRI images are often aligned to a standard "reference" coordinate system that is represented by an atlas. For cardiac [12] and brain MR imaging [13, 14], such atlases have been well established, and contributed significantly to the advancements of automated image segmentation and more sophisticated techniques for morphometric analysis while correcting for unrelated global anatomical variations among individuals [15–18]. In addition, they also formed the common ground for comparing and sharing research results. However, so far there has not been any atlas of similar nature for the assessment of lumbar paraspinal muscles.

In this article, we present the construction of a set of population-averaged unbiased atlases for axial MR images of the lumbar paraspinal muscles at the L4–L5 and L5–S1 levels. The atlases were established for three different age-groups (30–39 years old, 40–49 years old, and 50–59 years old) stratified by gender, as well as the entire cohort using both linear and nonlinear image registrations. They will provide the necessary reference coordinate spaces to help develop and conduct automated imaging analysis with improved efficiency for lumbar paraspinal muscles in relation to aging, LBP, and various lumbar pathologies.

Materials and methods

Subjects and imaging protocol

In total, 117 patients aged between 30 and 59 years old with commonly diagnosed lumbar pathologies were included in this study. These subjects were retrospectively selected from a larger sample of patients participating in the multi-center Genodisc project. Patient selection was done randomly and was stratified by age groups and gender. Only patients with good MRI quality were included. All patients provided informed consent, acknowledging that their data would be used for research on better understanding and characterizing common spinal disorders. The study was approved in Hungary by the Scientific and Research Ethics Committee of the Medical Research Council (431/PI/2007), as well as the local ethics committee of the institute, where the study was conducted. For atlas construction, the population was divided into three groups: 30–39, 40–49, and 50–59 years old, and for each group, 19–21 subjects were included for each of male and female cohorts. T2-weighted (T2w) MRI scans of the lumbar muscles were used for all patients, and axial slices of the L4–L5 and L5–S1 levels at mid-disc were acquired to make the final atlases since they are most often used in lumbar spinal pathology studies. All patient data were acquired in the supine position.

Image preprocessing

As the patient data were acquired at multiple medical centers, different MRI protocols and scanners have been used for scanning, resulting in different image resolution, image intensity range, and some discrepancies in image contrast. To unify these variations, all axial cross-sectional images were corrected for MRI intensity inhomogeneity due to non-uniform magnetic field in the scanner [19], and then image intensity standardization was performed using the technique introduced by Nyul et al. [20] so that each scan exhibits a unified image contrast and intensity range. Finally, all images were resampled to the same in-plane resolution of 0.33×0.33 mm^2.

Atlas construction

In general, two types of atlases (linear and nonlinear) were constructed using the preprocessed images. The linear atlases help define the general reference space, where the global body size differences were normalized with linear spatial transformations (translation, scaling, rotation, and shear), but with the individual morphometric features remained intact. The nonlinear version further reduces individual morphometric features by nonlinear image deformation from the linear version to form an atlas with well-delineated anatomy. To construct the linear atlases, all preprocessed images were co-registered (e.g., data were transformed into one coordinate system so that corresponding anatomical features were matched/aligned to each other) linearly using an algorithm [21] that intends to maximize the structural coherence among aligned images. The final atlas was formed by averaging all the linearly registered images. The nonlinear atlas follows the results of linear registration. Unbiased group-wise nonlinear registration using cross-correlation as the similarity metric [22] was performed for images after linear alignments, and the transformed results were averaged to form the atlas. To improve the image quality, left–right-mirrored images were used for both linear and nonlinear registrations, resulting in symmetric images. Here, Fig. 1 is included to help understand the atlas construction process.

Anatomical variations due to age and gender

To preliminarily demonstrate the potential applications of the reference space that the atlases offer, we performed linear and nonlinear registrations in the atlas space with respect to different schemes of subgrouping and compared their results. More specifically, in two different experiments, we regrouped the cohort with respect to gender and age, and visually inspected the differences potentially linked to these factors. For the age factor, the cohort was re-divided into the age groups of 30–39, 40–49, and 50–59 years old.

Results

Population-averaged atlases

The resulting linear and nonlinear versions of atlases for the entire cohort are shown in Fig. 2. As displayed in the figures, both atlases showed the averaged image features of the anatomy at the L4–L5 and L5–S1 levels, with the structures more well defined in the nonlinear versions. Due to the inclusion of left–right-mirrored images, the final atlases are symmetric. Compared with the individual MRI scans in Fig. 1, the atlases preserved the typical anatomy while largely reducing the individual differences in muscle shapes and composition, making them unbiased toward specific individual anatomical characters.

Anatomical variations due to gender and age

The averaged images after group-wise linear and nonlinear registrations with respect to gender are shown in Fig. 3. In addition, the muscle groups of each gender from nonlinear registration were contoured manually in different colors and overlaid on the population-averaged atlas from Fig. 2 for

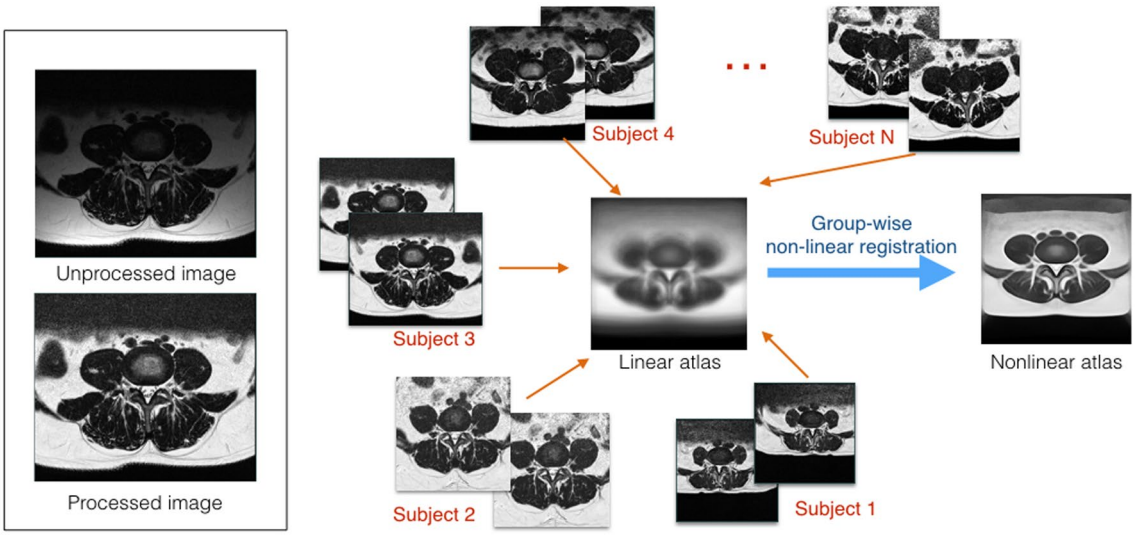

Fig. 1 Demonstration of atlas construction using L4–L5 cross-sectional MRI scans as an example. The comparison between before and after image preprocessing is shown on the left for an individual patient, and the process of atlas construction is illustrated on the right

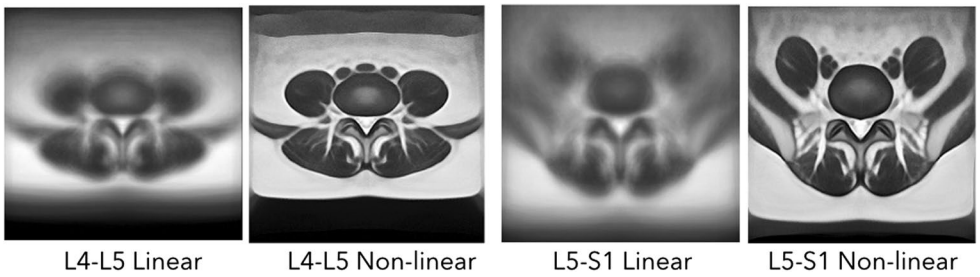

Fig. 2 Population-averaged linear and nonlinear atlases of the entire cohort for lumbar paraspinal muscles at L4–L5 and L5–S1 levels

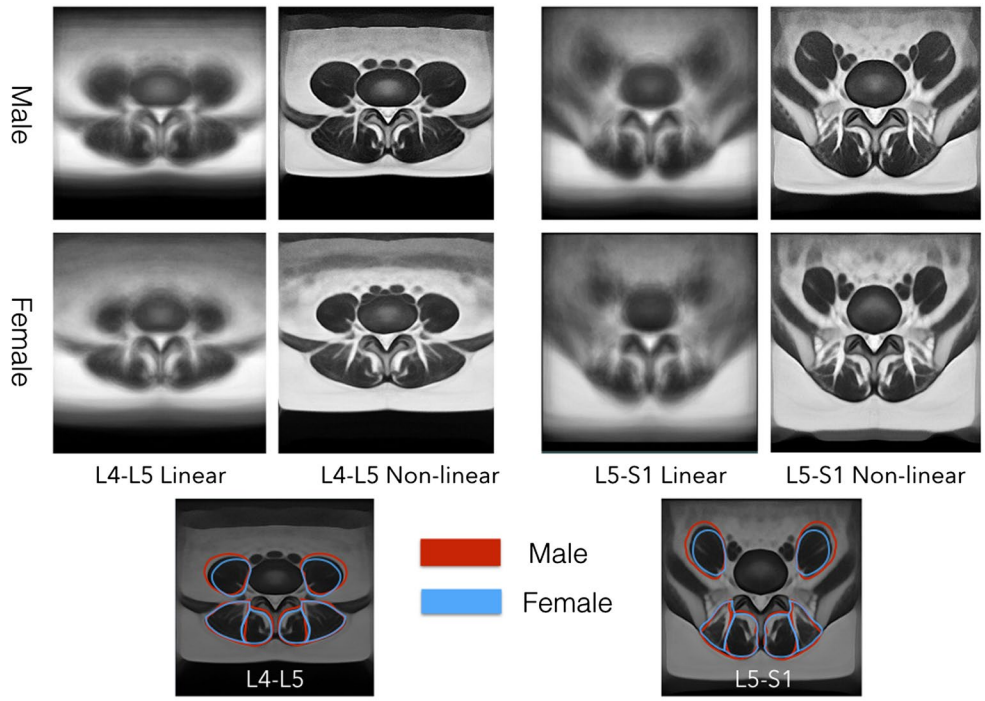

Fig. 3 Demonstration of anatomical variations with respect to gender with group-averaged images using linear and nonlinear registrations in the newly defined atlas coordinates. At the bottom, the contours of muscle groups for both genders were overlaid upon the population-averaged results of the entire cohort from Fig. 2

visual comparison. From both linear and nonlinear versions of the images, it can be observed that female subjects have more fatty infiltration in multifidus and erector spinae muscles at both spinal levels. From the overlaid muscle contours, we can see that the psoas muscle is larger for males. While the multifidus muscle of females is slightly wider in the lateral direction, it appears to be shorter in the anterior–posterior direction as compared to males. For the L4–L5 level, the erector spinae muscle is slightly larger for males than females.

The averaged images after group-wise linear and nonlinear registrations with respect to different age-groups are depicted in Fig. 4. From both linear and nonlinear registration results, we can observe that fatty infiltration increases with age and is more severe for the 50–59-year-old age-group. The paraspinal muscles resulting from the nonlinear registration of each age-group were also contoured manually in different colors and overlaid on the population-averaged atlas from Fig. 2 to allow comparison. From the muscle contours overlay, it can be observed that the shapes of multifidus and erector spinae muscles are similar across the three age-groups, while the size of psoas muscle appears larger in the 30–39-year-old group than in other groups.

Discussion

MRI atlases have been almost ubiquitously employed to aid neuro-image analysis. They provide the references that individual anatomy can be spatially normalized to, and are often used in two ways. First, by registering individual MRIs to the atlas, local tissue atrophy can be pinpointed from morphometric analysis [16, 23] by statistically comparing the resulting deformation fields or tissue density after the initial registration to compensate for global body size differences. Second, as multi-atlas label fusion [18] and convolutional

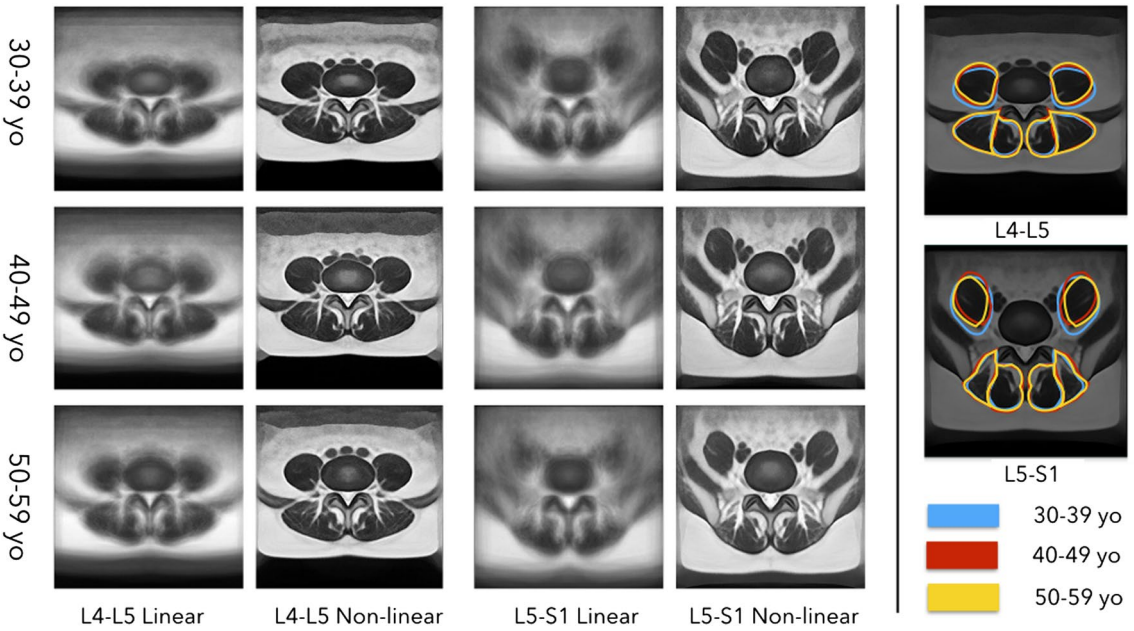

Fig. 4 Demonstration of anatomical variations with respect to age with group-averaged images using linear and nonlinear registrations in the newly defined atlas coordinates. On the right, the contours of muscle groups for all age-groups were overlaid upon the population-averaged results of the entire cohort from Fig. 2

neural networks [24] have become the "state of the art" for automatic brain image segmentation, individual alignment to the atlas space ensures the efficiency and accuracy of these algorithms. Automated image processing and analysis techniques by leveraging the power of MRI atlases have resulted in a large body of potential image-based biomarkers for neurological conditions. Similar MRI processing and analysis methods may very well benefit the research of LBP and other common spinal disorders.

To better represent the general population that is affected by LBP and related pathologies, we have included roughly equal numbers of patients in each of the three age-groups investigated, as well as for each gender. For this study, we used data from 117 patients to construct the atlases. Although it is widely accepted in brain imaging analysis that a larger cohort will enrich the representativeness of the atlas considering the publicly available ones containing various numbers of subjects [13, 14, 25], so far, we are aware of no determinations of the minimum sample size in relation to the variation, since the underlying variation can be complicated by many factors, and their characteristics are also under investigation. In this study, we demonstrated the technique of atlas construction using a cohort of patients with LBP, taking into account the following two considerations. First, there is a strong interest in characterizing the morphology (e.g., shape and size) and composition (e.g., fatty infiltration) of paraspinal muscles in this population. Second, lumbar-related pathologies have been associated with paraspinal muscle degenerative changes (atrophy, asymmetry, fatty infiltration) and thus are more challenging in terms of group-wise image alignment in atlas making, in comparison with healthy subjects. With precedence of the atlases in this article, we can easily adapt the proposed technique to construct similar atlases for healthy subjects in the future. The employed image registration methods for atlas making were not exclusively designed for brain analysis and can be used for many other structures by adapting the relevant parameters to accommodate the properties of the structures under study. The description of the full methodologies is described in [21, 22]. Since muscle asymmetry can occur on either side of the body, we decided to generate symmetric atlases using both the original and left–right-mirrored images. In addition, by increasing the total number of images for averaging from using mirrored images, the image quality and atlas representativeness can be further improved.

Overall, the observations from population-averaged images with respect to differences between genders agree with previous studies [9]. With respect to age, visual comparison shows that more fatty infiltration and atrophy of the psoas muscles occur in the 50–59-year-old group, and the differences between the 30–39- and 40–49-year-old groups are less pronounced. These observations follow the general trend of previous studies [5, 10]. It is important to note that these observations are confounded by the underlying pathologies, and further detailed investigations are necessary to decouple different factors with the help of image segmentation [15, 17, 18] or morphometric analysis techniques [23]. More particularly, for morphometric analysis, it is desirable

to match the characteristics of the atlas with the population under study [13] to reduce the morphological changes induced from unwanted factors. Therefore, in certain cases, age- or gender-specific atlases as demonstrated in this article can be used instead. However, comprehensive studies on muscle morphology and composition due to factors such as physical fitness or specific pathologies were not the focus of this work and are therefore out of the scope of the article. In the future, we will conduct more thorough studies using the resulting atlases from this work.

Conclusion

The proposed population-averaged atlases provide the standard imaging space data necessary for the development of automated image analysis algorithms, which would greatly simplify the tedious aspect of MR imaging assessment of paraspinal muscle morphometry and provide a standardized procedure to facilitate comparison among studies. Our preliminary results from the L4–L5 and L5–S1 levels with the image processing techniques demonstrated good results. We are now expanding this work to other lumbar spinal levels using larger samples to develop a fully automated atlas-based segmentation algorithm.

Acknowledgement This project was partly funded by the Natural Sciences and Engineering Research Council of Canada (NSERC) Discovery Grant RGPIN-2015-04136.

Compliance with ethical standards

Conflicts of interest The authors declare that they have no conflict of interest.

Ethical approval All procedures performed in studies involving human participants were in accordance with the ethical standards of the institutional and/or national research committee and with the 1964 Declaration of Helsinki and its later amendments or comparable ethical standards.

Informed consent Informed consent was obtained from all individual participants included in the study.

References

1. Balague F, Mannion AF, Pellise F, Cedraschi C (2012) Non-specific low back pain. Lancet 379(9814):482–491. https://doi.org/10.1016/S0140-6736(11)60610-7
2. Deyo RA, Weinstein JN (2001) Low back pain. N Engl J Med 344(5):363–370. https://doi.org/10.1056/NEJM200102013440508
3. Refshauge KM, Maher CG (2006) Low back pain investigations and prognosis: a review. Br J Sports Med 40(6):494–498. https://doi.org/10.1136/bjsm.2004.016659
4. Zotti MGT, Boas FV, Clifton T, Piche M, Yoon WW, Freeman BJC (2017) Does pre-operative magnetic resonance imaging of the lumbar multifidus muscle predict clinical outcomes following lumbar spinal decompression for symptomatic spinal stenosis? Eur Spine J 26(10):2589–2597. https://doi.org/10.1007/s00586-017-4986-x
5. Shahidi B, Parra CL, Berry DB, Hubbard JC, Gombatto S, Zlomislic V, Allen RT, Hughes-Austin J, Garfin S, Ward SR (2017) Contribution of lumbar spine pathology and age to paraspinal muscle size and fatty infiltration. Spine 42(8):616–623. https://doi.org/10.1097/BRS.0000000000001848
6. Hodges P, Holm AK, Hansson T, Holm S (2006) Rapid atrophy of the lumbar multifidus follows experimental disc or nerve root injury. Spine 31(25):2926–2933. https://doi.org/10.1097/01.brs.0000248453.51165.0b
7. Yarjanian JA, Fetzer A, Yamakawa KS, Tong HC, Smuck M, Haig A (2013) Correlation of paraspinal atrophy and denervation in back pain and spinal stenosis relative to asymptomatic controls. PM&R 5(1):39–44. https://doi.org/10.1016/j.pmrj.2012.08.017
8. Ranger TA, Cicuttini FM, Jensen TS, Peiris WL, Hussain SM, Fairley J, Urquhart DM (2017) Are the size and composition of the paraspinal muscles associated with low back pain? A systematic review. Spine J 17(11):1729–1748. https://doi.org/10.1016/j.spinee.2017.07.002
9. Takayama K, Kita T, Nakamura H, Kanematsu F, Yasunami T, Sakanaka H, Yamano Y (2016) New predictive index for lumbar paraspinal muscle degeneration associated with aging. Spine 41(2):E84–E90. https://doi.org/10.1097/BRS.0000000000001154
10. Fortin M, Videman T, Gibbons LE, Battie MC (2014) Paraspinal muscle morphology and composition: a 15-year longitudinal magnetic resonance imaging study. Med Sci Sports Exerc 46(5):893–901. https://doi.org/10.1249/MSS.0000000000000179
11. Fortin M, Omidyeganeh M, Battie MC, Ahmad O, Rivaz H (2017) Evaluation of an automated thresholding algorithm for the quantification of paraspinal muscle composition from MRI images. Biomed Eng Online 16(1):61. https://doi.org/10.1186/s12938-017-0350-y
12. Young AA, Frangi AF (2009) Computational cardiac atlases: from patient to population and back. Exp Physiol 94(5):578–596. https://doi.org/10.1113/expphysiol.2008.044081
13. Fonov V, Evans AC, Botteron K, Almli CR, McKinstry RC, Collins DL, Brain Development Cooperative G (2011) Unbiased average age-appropriate atlases for pediatric studies. Neuroimage 54(1):313–327. https://doi.org/10.1016/j.neuroimage.2010.07.033
14. Xiao Y, Fonov V, Beriault S, Al Subaie F, Chakravarty MM, Sadikot AF, Pike GB, Collins DL (2015) Multi-contrast unbiased MRI atlas of a Parkinson's disease population. Int J Comput Assist Radiol Surg 10(3):329–341. https://doi.org/10.1007/s11548-014-1068-y
15. Cabezas M, Oliver A, Llado X, Freixenet J, Cuadra MB (2011) A review of atlas-based segmentation for magnetic resonance brain images. Comput Methods Programs Biomed 104(3):e158–e177. https://doi.org/10.1016/j.cmpb.2011.07.015
16. May A, Gaser C (2006) Magnetic resonance-based morphometry: a window into structural plasticity of the brain. Curr Opin Neurol 19(4):407–411. https://doi.org/10.1097/01.wco.0000236622.91495.21
17. Xiao Y, Bailey L, Chakravarty MM, Beriault S, Sadikot AF, Pike GB, Collins DL (2012) Atlas-based segmentation of the subthalamic nucleus, red nucleus, and substantia nigra for deep brain stimulation by incorporating multiple MRI contrasts. Paper presented at the Proceedings of the third international conference on Information Processing in Computer-Assisted Interventions, Pisa, Italy
18. Xiao Y, Fonov VS, Beriault S, Gerard I, Sadikot AF, Pike GB, Collins DL (2015) Patch-based label fusion segmentation of brainstem structures with dual-contrast MRI for Parkinson's

disease. Int J Comput Assist Radiol Surg 10(7):1029–1041. https://doi.org/10.1007/s11548-014-1119-4
19. Tustison NJ, Avants BB, Cook PA, Zheng Y, Egan A, Yushkevich PA, Gee JC (2010) N4ITK: improved N3 bias correction. IEEE Trans Med Imaging 29(6):1310–1320. https://doi.org/10.1109/TMI.2010.2046908
20. Nyul LG, Udupa JK, Zhang X (2000) New variants of a method of MRI scale standardization. IEEE Trans Med Imaging 19(2):143–150. https://doi.org/10.1109/42.836373
21. Peng YG, Ganesh A, Wright J, Xu WL, Ma Y (2012) RASL: robust alignment by sparse and low-rank decomposition for linearly correlated images. IEEE Trans Pattern Anal 34(11):2233–2246. https://doi.org/10.1109/Tpami.2011.282
22. Avants BB, Tustison NJ, Song G, Cook PA, Klein A, Gee JC (2011) A reproducible evaluation of ANTs similarity metric performance in brain image registration. Neuroimage 54(3):2033–2044. https://doi.org/10.1016/j.neuroimage.2010.09.025
23. Ashburner J, Hutton C, Frackowiak R, Johnsrude I, Price C, Friston K (1998) Identifying global anatomical differences: deformation-based morphometry. Hum Brain Mapp 6(5–6):348–357
24. Litjens G, Kooi T, Bejnordi BE, Setio AAA, Ciompi F, Ghafoorian M, van der Laak JAWM, van Ginneken B, Sanchez CI (2017) A survey on deep learning in medical image analysis. Med Image Anal 42:60–88. https://doi.org/10.1016/j.media.2017.07.005
25. Shattuck DW, Mirza M, Adisetiyo V, Hojatkashani C, Salamon G, Narr KL, Poldrack RA, Bilder RM, Toga AW (2008) Construction of a 3D probabilistic atlas of human cortical structures. Neuroimage 39(3):1064–1080. https://doi.org/10.1016/j.neuroimage.2007.09.031

Affiliations

Yiming Xiao[1] · Maryse Fortin[2] · Michele C. Battié[3,4] · Hassan Rivaz[2,5]

1 Robarts Research Institute, Western University, 1151 Richmond Street North, London, ON N6A 5B7, Canada

2 PERFORM Centre, Concordia University, Montreal, Canada

3 School of Physical Therapy, Western University, London, Canada

4 Bone and Joint Institute, Western University, London, Canada

5 Department of Electrical and Computer Engineering, Concordia University, Montreal, Canada